Shape optimization of a loudspeaker diaphragm with respect to sound directivity properties

by

S!Ziren T. Christensen and Niels Olhoff

Institute of Mechanical Engineering, Aalborg University,
Pontoppidanstraede 101, DK-9220 Aalborg East, Denmark

Abstract: This paper presents a novel method for optimizing the directivity of the sound emission from the diaphragm of an electro dynamic loudspeaker. The analysis of the diaphragm is performed by finite element analysis of the structural dynamic behaviour and using the boundary element method for the acoustic analysis. Through optimization of a dead mass distribution on the diaphragm, or of the shape of the mid-surface of the diaphragm, it has been possible to improve its directivity properties for sound emission. Several illustrative examples are presented at the end of the paper.

Keywords: Acoustics, loudspeaker sound directivity, optimum design, finite element method, boundary element method

1. Introduction

An ideal diaphragm would have a piston-like behaviour with a variable, frequency dependent radius. This is obviously not possible with an ordinary loudspeaker unit where the radius is fixed, and the diaphragm only behaves as a piston in the lower part of its frequency range. This is the reason why a typical loudspeaker has several units of different radii, in order to cover the entire audible frequency range.

Modern loudspeaker units exhibit good mechanical and acoustic behaviour, but only within a specific frequency range, which is due to the physical behaviour of the diaphragm "breaking up" when the excitation frequency exceeds a threshold value. At the same time, while the sound radiation is uniform in all directions when the frequency is in the lower part of its range, the diaphragm has a tendency to radiate within a more narrow angle for increasing excitation frequencies. This is caused by interference phenomena that occur when the sound wave length in the air becomes equal to or larger than the circumferential distance of the diaphragm. This naturally leads to the idea of designing a

diaphragm which has a frequency dependent effective radius, i.e., to perform an optimization of the diaphragm design with a view to decouple the outer parts of the diaphragm for frequencies above the threshold value. Such an approach was taken by Vollesen (1994), who formulated a mechanical objective function for the optimization which was based on a frequency dependent decoupling of the diaphragm. However, due to problems concerning differentiability of the objective function, definitive optimum designs were not obtained.

Several formulations of objective functions have been investigated in this paper: first a mechanical objective function based on a frequency dependent effective radius was tried, then an acoustic objective function based on the energy flux from the diaphragm was formulated, but both failed in being able to make the directivity uniform. Finally, an objective function directly based on the attainment of a desired directivity diagram was formulated and led to successful results.

Three different types of axisymmetric design models have been investigated in this paper, first a flat circular diaphragm with the design variables taken to be the masses and radial positions of a set of concentric, dead ring masses attached to the diaphragm. Secondly, we applied a design model taking the shape of the mid-surface of a membrane of constant thickness as design variable, describing the surface by a quadratic B-spline. Finally, we used a design model similar to the previous one, but based on a cubic spline and inserted in a soft surround, with consideration that both the diaphragm and the surround have a variable thickness. Furthermore, both single and multiple frequency optimizations have been performed for these types of design model.

In order to be able to perform the optimization, a structural-acoustic coupled combination of the Finite Element (FE) and the Boundary Element (BE) methods has been used. The BE code has been implemented in the general optimum design system ODESSY which is being developed at Aalborg University and makes it possible to use a wide range of design variables, see Lund (1994) and Rasmussen et al. (1993).

2   Acoustic analysis

The acoustic analysis is performed by using the BE method based on the Helmholtz integral in the following form, see Sorokin (1995), Wu, Seybert and Li (1993), and Brebbia (1991) (an axisymmetric formulation may be found in M0ller, 1993 or Soenarko, 1993),

$$C(P)\, p(P) \;=\; \int_S (p(Q)\partial R) - \; + \; iwpavn(Q)G(R))\, dS \tag{1}$$

Here, $p(P)$ is the acoustic pressure at the point P, $v_n(Q)$ is the normal velocity at the point Q of the structural surface S with the unit normal vector n and it is assumed that $p(Q)$ and $p(P)$ satisfy the Helmholtz wave equation $\nabla^2 p + k^2_p = 0$ for time harmonic waves, where $k = \frac{\omega}{c}$ denotes the wavenumber,

c and w denote the speed of sound in the acoustic medium and the angular frequency, respectively. The function $G(R)$ is the free-space Green's function, $G(R) = \frac{e^{-i\frac{R}{c}}}{R}$, where R is the distance between the points P and Q and the coefficient $C(P)$ is the space-angle at the observation point.

The procedure consists in subdividing the surface of the structure into N elements and to make a discretization of the Helmholtz integral. This makes it possible to set up a system of equations for the relationship between the surface pressure and the displacement. The system of equations is set up to formulate the coupled structural acoustic problem. First, equations are formulated by letting the points P be the nodal points on the surface. For a single node [i] the pressure can then be found as the sum of contributions from all the finite elements. By setting up this equation for all the N nodes, the following system of equations is formed

$$C(P)p(P) = \sum^{N} \int_{e} \frac{\partial G}{\partial n}(Pi, Q)\, p\, dS(Q) - \sum^{N} \int_{e} G(\bar{P}i, Q)\, p_o\, w^2\, u_n\, dS(Q) \quad (2)$$

where $v = iwu$ has been inserted.

In the following a new notation for the acoustic equations and an axisymmetric formulation of (1) is introduced, see Moller (1993) or Soenarko (1993).

$$A = C(P) - \sum_{j=1}^{\prime} \int_{Ie} \int_0^2 \frac{\partial G}{\partial n}(Pi, Q)\, d\theta(Q)r(Q)dL(Q) \quad (3)$$

$$B = - \sum_{j=1}^{\prime} \int_{Ie} \int_0^2 G(\bar{P}i, Q)\, p_o\, w^2\, d\theta(Q)r(Q)dL(Q) \quad (4)$$

Now the equation system giving the relation between surface pressures p and normal components of the displacement amplitudes Un is expressed as

$$A\,p = B\,Un \quad (5)$$

where the influence matrices A and B are fully populated, complex, and non-symmetric.

The structural equation in finite element form is found to be

$$(K(nxn) - w^2 M(nxn) + i\,w\,c(nxn))\, u(nxl) = fm(nxl) + f^a(nxl) \quad (6)$$

where f^a denotes the fluid pressure load on the structure. When this equation is combined with the relation between surface pressure and normal displacement in (5), we have the following system of equations (Seybert, Wu and Li, 1991) which expresses the coupling between the finite element (FE) model and the boundary element (BE) analysis:

$$\begin{bmatrix} K(nxn) - w^2 M(nxn) + i\,w\,c(nxn) & L(nxl) \\ -B(lxl)^{T} r^{(lxn)} & A(lxl) \end{bmatrix} \begin{Bmatrix} u(nxl) \\ p(lxl) \end{Bmatrix} = \begin{Bmatrix} fm(nxl) \\ o(lx1) \end{Bmatrix} \quad (7)$$

Here, K, M a n d C denote the global stiffness, mass, and damping matrices of
the vibrating structure. The matrix T r executes the transition from the total
number of structural degrees of freedom n to the number of degrees of free-
dom l represented by the normal displacement amplitudes used in the acoustic
analysis, by projection of the displacement amplitude vector onto the normal
vector. L denotes the fluid/structure coupling matrix, and is used to find the
force vector f^a which the fluid pressure generates on the surface,

$$-L(nxl)\ p(lx1)\ =\ f^a\ (nxl) \tag{8}$$

The sizes of the vectors are described in terms of n structural degrees of freedom,
the number m of modes used in the analysis, and l which denotes the number
of surface nodes.

2.1. Eigenvector synthesis technique

By using the eigenvector synthesis technique it is possible to reduce the size of
the system of equations (7), see Wu, Seybert and Li (1991). The displacement
u can be approximated by a linear combination of the eigenvectors S for the
undamped system, i.e., the structure in vacuum. Another possibility would have
been to use Ritz or Lanczos vectors instead of eigenvectors, which would make
it possible to reduce the number of vectors further due to the smaller number
of vectors to be used, see Jeans and Mathews (1991), or Seybert, Wu and Li
(1991). The displacement vectors u can thus be expressed as

$$U(nxl)\ =\ S^{(nxm)}\ _{>,s}^{(mxl)} \tag{9}$$

where A_s denotes the participation vector, describing the participation from
each eigenvector to the overall displacement, and m denotes the number of
eigenvectors used in the approximation.

   It is now possible to write the system of equations as follows, where the
number of DOF is reduced substantially compared to the initial problem:

$$\begin{bmatrix} K(mxm) & -w2\,M(mxm) + i\,w\,c(mxm) & L(nxl)] \\ & -B(mxm)_{ss} & A(lxl) \end{bmatrix} \left\{ \begin{matrix} A(mx\,1) \\ p(lxl) \end{matrix} \right\} = \left\{ \begin{matrix} f_m\ (mx\,1)\} \\ o(lxl) \end{matrix} \right\} \tag{10}$$

If the eigenvectors S are orthonormalized with respect to the mass matrix M
and Rayleigh damping is used, we have $C = a\,M + \beta\,C$, where a and β are
constants. By introducing the modal damping ratio (i $=$ ½(;:,- + Wi (3),
we can find the matrices in (10) as

$$K(mxm)_{ss} = [''-2]_{w\,r}(mxm) \qquad Min;'xm) = [.'''--himxm)$$
$$c(mxm)_{ss} = [.\ w;t;i''.\ ](mxm) \qquad B(mxm)_{ss} = s\,T\ (mxl)\,B(lxl)\,s(lxm)$$

Now the following equation can be derived for determination of the participation vector for each of the given eigenvectors by inserting p = A -^{1} $\boldsymbol{BTru}$ in the structural part of (10):

$$[(K(\underset{ss}{m}xm) - w^2 M(\underset{ss}{m}xm) + i\,w\,c(\underset{ss}{m}xml) +$$

$$\left(sT_{(mxn)\,L(nxl)}A^{-1}(lxl)B(lxl)s\,xm))\right] \quad \{A\,\ddot{i}\ddot{m}xl)\} \;=\; \boldsymbol{\mathcal{t}:}_{\mathnormal{i}}(mxl)\} \quad (11)$$

When the participation vector is found, it may be used for finding the pressure using (9) and p = A-l BTru. Having determined both the surface pressure and the displacement vectors, we can determine the pressures in the acoustic medium by using (1). This is done by writing a new set of the equations and calculating the integrals corresponding to the points chosen in the acoustic medium. Thus, no system of equations needs to be solved; the pressures can be found by multiplication of the new integrals by the surface pressures and displacements.

3.   Optimization

In order to select an effective objective function, differently formulated objective functions were considered for optimizing a distribution of dead ring masses on flat membranes. The reason for choosing a flat structure for this investigation was to be able to explain and verify that the design determined was actually optimum, and to understand the mechanism which gives a uniform directivity.

The following objective functions were investigated: first a mechanical objective function based on a frequency dependent effective radius was tried, and then an acoustic one based on the energy flux from the diaphragm, but both failed in being able to render the directivity uniform. Finally, an objective function directly based on the directivity diagram was formulated, and it made it possible to obtain a uniform directivity for a flat membrane.

This objective function was taken to be the sum of the p-norms of the differences between a prescribed target pressure and the actual sound pressure at a number of N points, n = 1, .. N lying on a circle with a radius of 3 m from the center of the diaphragm, which is the usual distance applied for sound pressure, see Fig. 1 and (12),

$$f(\{a\}) \;=\; \boldsymbol{L}_{n=1}^{N} \, (R_{:}^{:} \,-\, R\,t \qquad (12)$$

where $R'_:$, and R , are respectively, the desired and the obtained sound pressure values at the points n, n=1,...,N, and {a} is the vector of design variables.

The design variables for the first design problem to be considered in this paper are taken to be the masses m_i and the radial positions r_i, i = 1, ... ,I, of a set of concentric, dead ring masses attached to the diaphragm, i.e., the vector
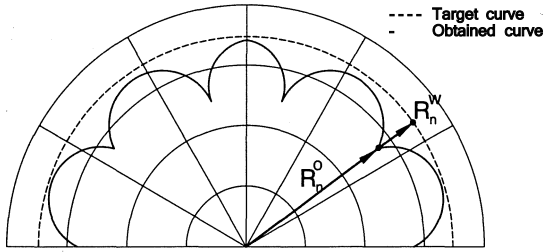
Figure 1. The principle of the objective function

of design variables is $\{a\} = \{m1, ..., m1, r1, ..., r1\}^T$, and the optimization problem is formulated mathematically as

$$\min[J(\{a\}) = \sum_{n=1}^{N} (R''_{::} - R\,Y] \tag{13}$$

subject to:

$$\sum_{i=1}^{I} m i 2'. \quad M$$

$$0 \leq mi \leq mf \qquad i = 1, ..., I$$

$$0 \leq ri \leq A \qquad i = 1, ... J$$

Here, the first constraint specifies a total mass M of the ring masses which is a minimum allowable value when the targeted dB level is larger than the dB level of the initial and the optimized diaphragm. Normally, this constraint is only active during the first iterations. The subsequent constraints are simple side constraints on the design variables, where m f are given upper values for the individual masses, and A denotes the outer radius of the diaphragm.

As will be reported in Section 4, first a design model consisting of a flat plate with an initially uniform distribution of discrete ring-masses attached to the surface is investigated in order to study a mechanism which may give a uniform directivity. These investigations show that it is possible to obtain a nearly uniform directivity for a flat membrane in the whole audible frequency range. This is achieved by placement of large ring masses in the inner part of the diaphragm which makes the diaphragm work as a point source by practically decoupling the outer parts of the membrane at high frequencies. Furthermore, a multifrequency analysis is performed in Section 4 which leads to an increase of the frequency interval in which the uniform directivity can be maintained at the same sound pressure level as that of the design optimized for a single frequency.

In Section 5, a second type of design model will be considered. In this design model, the shape of the mid-surface of the diaphragm is taken as a

design variable, and described by a quadratic B-spline. The B-spline is defined by 9 points where 8 of the points may move vertically, see Figs. 11 or 17. The design variables for this model are the positions of the points described through point modifiers k   The optimization problem based on this design model is formulated as

$$\min[f(\{a\}) \quad = \quad \sum_{n=l}^{N} (R'_{-}: \quad - \quad R \ ?l \tag{14}$$

subject to:

$$\textit{tl} \quad \text{Ji} \leq \textit{ft} \qquad i = 1, \dots, \textit{I}$$

where the point modifiers Ji are subjected to the lower and upper side contraints values $\textit{ff}$ and $\textit{ft}$.

The underlying structural acoustic analysis for the optimization problems is carried out as described in the foregoing, Due to the complexity of the problems, the sensitivity analysis of the objective function with respect to the design variables is performed by a simple finite difference approach, and a method of sequential linear programming is used for the optimization.

The investigations based on the design model in Section 5 confirm the results found in Section 4, namely that in order to obtain uniform directivity, the diaphragm area which radiates sound should be restricted in size.

In Section 6, a third design model is investigated, where the diaphragm considered is an axisymmetric shell with a soft surround. Here, the design variables are taken to be 8 modifiers defin'ing a cubic B-spline that represents the shape of the mid-surface of the diaphragm. Furthermore, the thicknesses of the shell and of the surround are used as design variables. Using this model in Section 6, it is again shown that it is possible to obtain uniform directivity through a multifrequency optimization.

4.   Example: Optimization of masses

The diaphragm is first considered as a flat, uniform circular elastic plate modelled with Mindlin axisymmetric elements (see Cook, 1974, and Tessler, 1982) to which a set of circular, concentric dead ring masses are attached. The radii and the magnitudes of these ring masses are adopted as design variables. For this flat plate structure the first term of the Helmholtz integral in (2) vanishes, and the integral reduces to Rayleigh's integral where the space angle C(p) is set to 2n due to the presence of an infinity large rigid baffie. It should be mentioned that the use of discrete masses for control of acoustic properties has been demonstrated by St. Pierre and Koopmann (1995) for the different problem of reducing the sound power radiation from plates by attaching optimally sized discrete masses to the plates, similarly, Lamancusa (1993), used the thickness of plates for a close formulation.
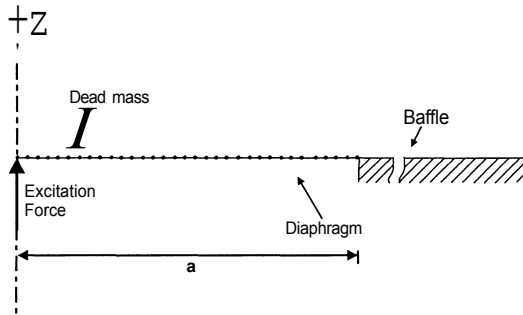
Figure 2. Design model for flat circular diaphragm with attached ring masses

Fig. 2 shows the design model where 32 ring-formed dead masses are attached to a circular clamped plate exited by a central, harmonically varying point force $f(t) = Ae^{iwt}$ with $A = lN$. The data for the design model can be seen in Table 1.

Material data		Model data	
Young's Modulus E	1.5E9 N/m^2	Plate thickness h	0.5 *mm*
		Plate radius a	40 m m
Density p	600 kg/m^3	Number of elements m	100
Poisson's ratio v	0.3		
Damping parameter	0.01		

Table 1. Model data

Firstly, the present design model was investigated for an excitation frequency of 10,000 Hz which results in a very directive pattern. The target value for the sound pressure at the semi-circle of radius 3 m from the membrane, was taken to be 90 dB. This value was chosen to be higher than the medium value for the sound pressure level at the corresponding semi-circle of the initial design, in order to make the optimized design radiate efficiently. In principle, the formulation of the objective function allows the target sound pressure to be chosen arbitrarily along any closed curve in front of the membrane. Fig. 3 shows the directivity pattern for a flat diaphragm plate, both for an initially uniform distribution of the discrete masses, and after the optimization of the discrete masses has been performed. It is clearly seen that the optimized directivity curve is much more uniform than the initial one. The target curve for the optimization is also shown in Fig 3.

Figs. 5 and 4 show, respectively, the optimum discrete mass distribution, and the modulus of the structural velocity as a function of the radial distance before
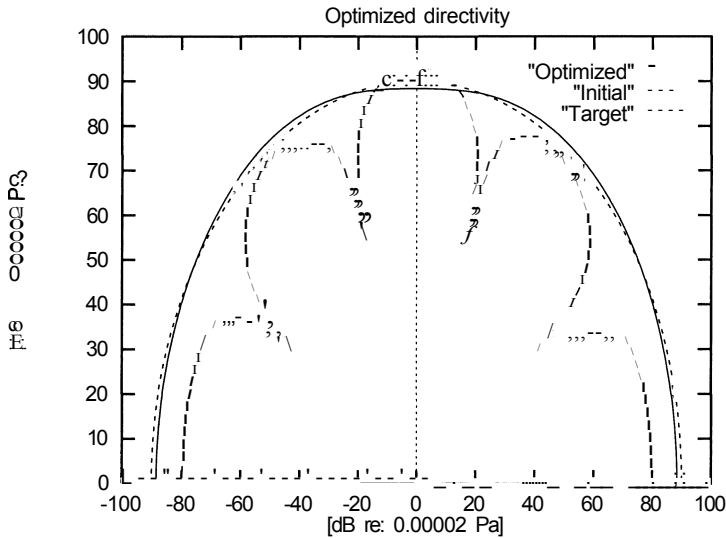
Figure 3. Directivity pattern initially and after optimization at 10,000 Hz (with respect to a target level of 90 dB)

and after the optimization. It is seen that the ring masses are located along nodal circles. Small masses are found near the center at the radius of 0.005 mm and introduce the first nodal circle, while large masses are located at larger radii.

The two velocity plots in Fig. 4 clearly illustrate that for the optimized design, the vibration amplitudes of the outer parts of the membrane are decreased, while the vibration amplitudes of the inner parts have been increased. This is closely connected with the discrete ring mass distribution which has a first large value at the radius of 0.0135 m, and after this distance the amplitudes of vibrations are reduced.

Fig. 6 shows the energy flux, scaled to unity, plotted as a function of the radial distance, both for the initial and for the optimized design. It is clearly seen that the energy flux from the optimized design is concentrated near the center of the membrane, while almost no flux is radiated from the outer part. The flux distribution explains the uniformity of the directivity diagram for the optimum design: since the flux is concentrated near the center, the membrane acts like a point source, which is always characterized by uniform directivity.

Another way of explaining this behaviour is that the concentrated flux makes interference phenomena unlikely to occur because the size of the area which radiates sound is small compared to the sound wave length in air. (As is well-known, it is interference phenomena which cause the narrow dips in directivity diagrams, viz. the curve for the initial design in Fig. 3).
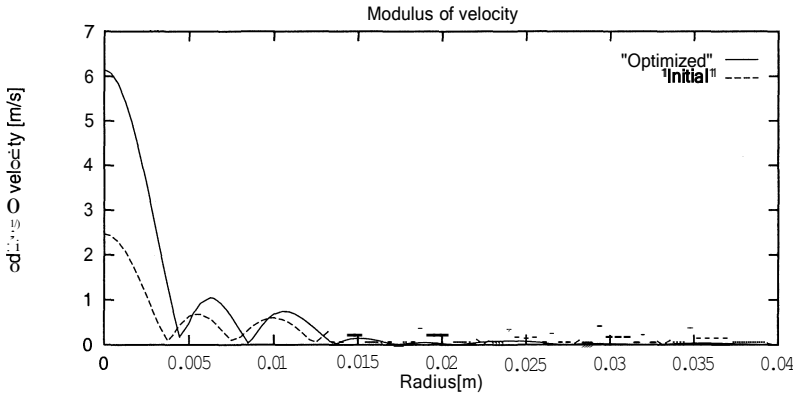
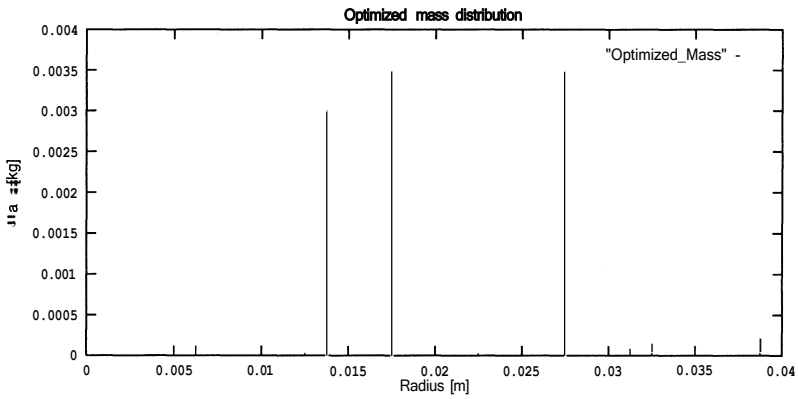Figure 4. Modulus of velocity before and after optimization at 10000 Hz

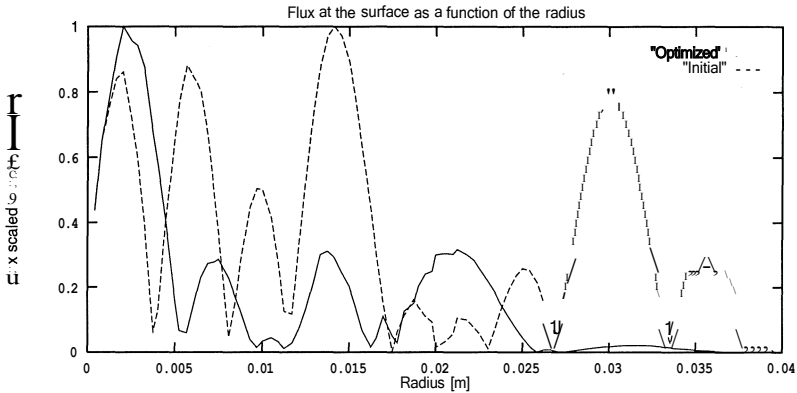Figure 5. Optimized mass distribution (initial distribution uniform).

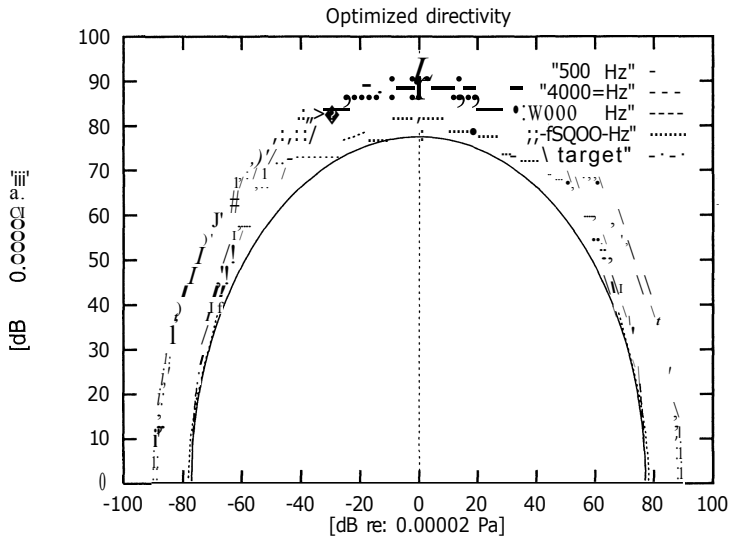Figure 6. Flux scaled to unity, inital and after optimization

Optimized directivity

Figure 7. Directivity patterns for single frequency optimized design subjected to different frequencies

Although the structure is optimized for just one frequency of 10,000 Hz, it maintains a uniform directivity over a wide frequency range spanning over several eigenfrequencies. This can be seen from Fig. 7 which shows the directivity diagram for the obtained design when subjected to excitation frequencies smaller and larger than 10,000 Hz. Here it is seen that the directivity remains uniform for all the frequencies, but that the sound pressure levels are different for the different excitation frequencies (the signatures for the curves indicate the excitation frequencies).

An experience gained from the optimization is that it is advantageous to perform the optimization stepwise, by starting with a low value of the excitation frequency for which the response yields a uniform directivity, and then increase the frequency in small steps until the frequency of interest is reached. By using this procedure, it is possible to avoid the occurrence of the narrow dips in the sound pressure level which are seen on the curve in Fig. 3 corresponding to the initial design.

In order to widen the frequency range for which the design maintains the uniform directivity, a multifrequency optimization was carried out using the same design model, but optimizing simultaneously for the excitation frequencies 500 Hz, 10000 Hz and 15000 Hz. The reasons for choosing the low frequency of 500 Hz for which the directivity can be expected to be uniform, is that this to a certain extent will ensure that the sound pressure levels for low frequencies are not lowered by optimization, which is often found to be the case when the
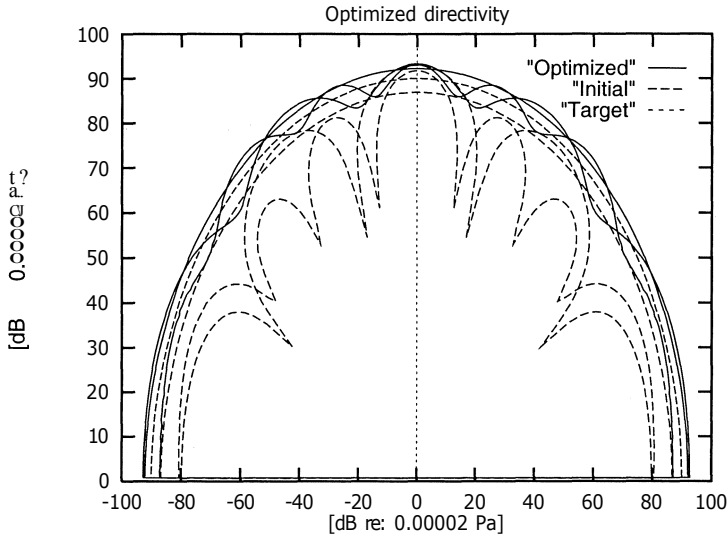
Optimized directivity

Figure 8. Directivity patterns initially and after multifrequency optimization at 500, 10,000 and 15,000 Hz (with respect to a target level of 90 dB)

design is optimized for a single high excitation frequency. This phenomenon can be seen in Fig. 7, where the directivity curve for 500 Hz corresponds to a lower sound pressure level.

For the multifrequency optimization problem, the objective function is simply defined as the sum of the three individual single frequency objectives, see (12). The result of the multifrequency optimization problem is presented in Fig. 8 which shows the directivity patterns for the three different frequencies initially and after the optimization. As is seen it has been possible to obtain a nearly uniform directivity at the same sound pressure level for the three frequencies.

If the multifrequency optimized design is subjected to frequencies for which it is not optimized, the behaviour naturally can be expected to be better than that of the single frequency optimized design; this can be seen by comparing Fig. 7 and Fig. 9. However, it is possible to excite the diaphragm by frequencies such that the uniformity of the directivity of the diaphragm is lost; this problem may be solved by using more frequencies in the optimization.

The mass distribution for the multifrequency optimum design example is shown in Fig. 10, and it is seen that the masses are basically distributed as in the case of the design optimized for a single frequency, with a large mass near the center, but whereas the single frequency design had three large masses the multifrequency design only has one large mass. This is due to the inclusion of the low frequency of 500 Hz in the multifrequency optimization problem.
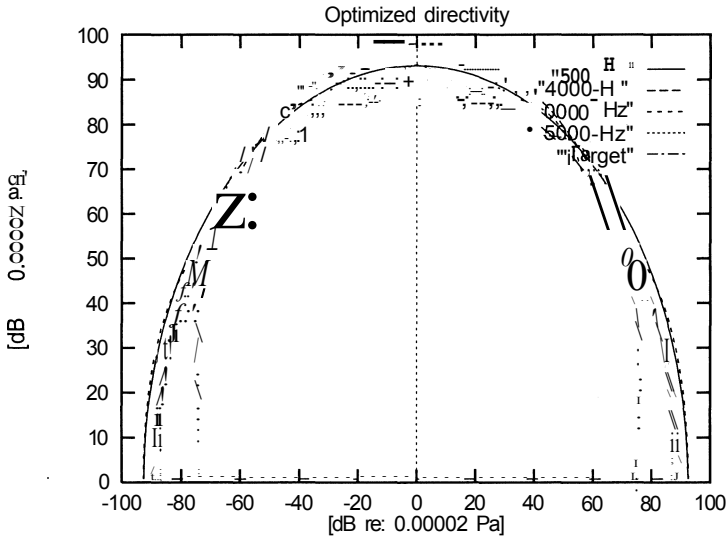
Figure 9. Directivity patterns for multifrequency optimized design subjected to additional frequencies
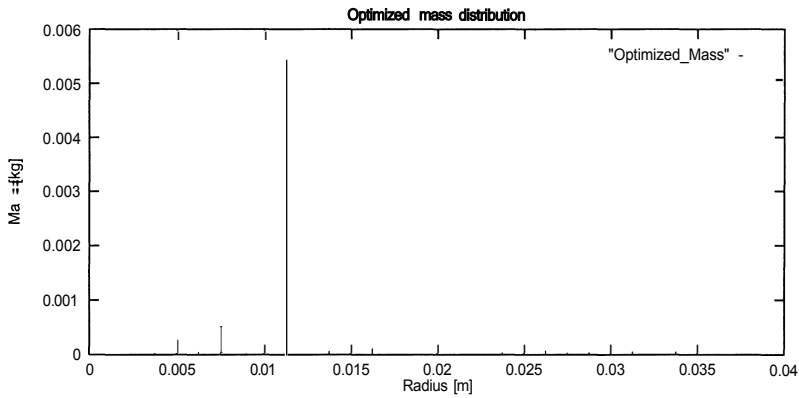

Figure 10. Optimized mass distribution on multifrequency optimized plate
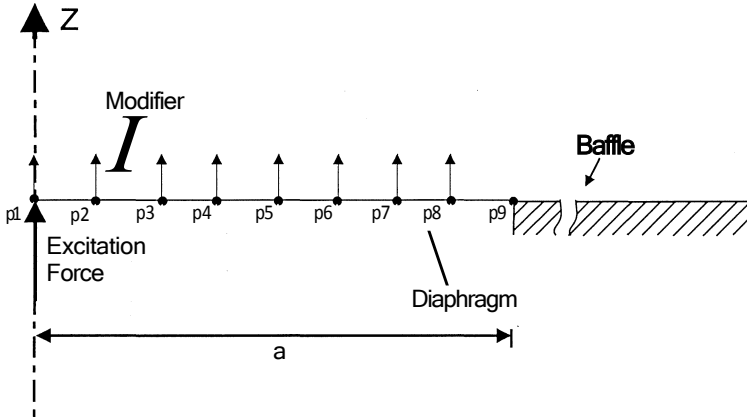
Figure 11. Design model for axisymmetric diaphragm with shape of mid-surface as a design variable

5. Example: Shape optimization

The second design model to be investigated is an axisymmetric elastic shell of constant thickness which is modelled by means of Mindlin axisymmetric shell elements.

The design variables are taken to be 8 modifiers defining the shape of a quadratic B-spline spanned by 9 points, governing the shape of the mid-surface of the diaphragm. Using the shape as a design variable requires full formulation of the Helmholtz integral, since now the first term will no longer vanish, and also the baffie needs to be discretized. The design model can be seen in Fig. 11. The data for the design model are the same as in the previous example except for the discretization of the baffie, and the design model is again excited by a central, harmonically varying point force $j(t) = Ae^{iwt}$ with A = lN and a frequency of 10,000 Hz.

The motivation for choosing the shape of the mid-surface as a design variable is that we pursue to demonstrate similarities between the optimum designs for two different design models, and this way verify the relevance of the found optima. In addition, we believe that the shape is a more practical design variable than discrete masses.

The result of the single frequency optimization is shown in Fig. 12, together with the directivity plot for the initial design and the target curve which is again taken to represent a target level of 90 dB.

The figure shows that the directivity is improved significantly corn.pared to the initial design. The optimized shape of the diaphragm mid-surface as a function of the radial coordinate is shown in Fig. 13, with the center-axis located at the left hand side.
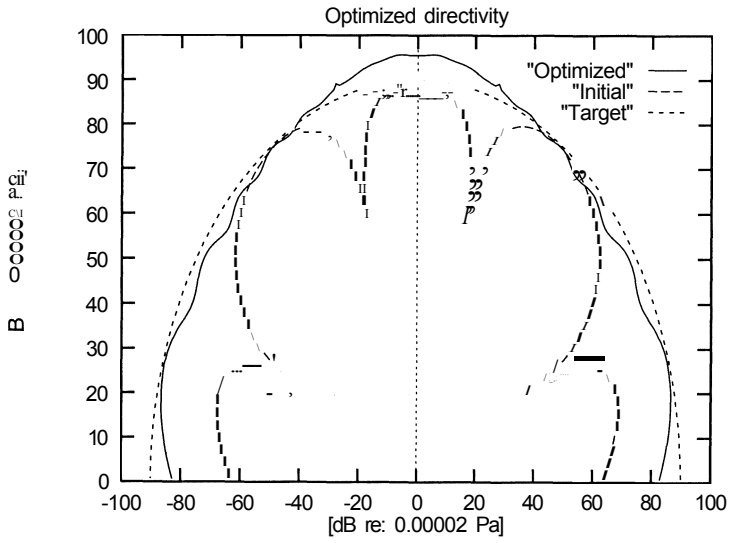
Optimized directivity

Figure 12.   Directivity pattern initially and after optimization at 10,000 Hz (with respect to a target level of 90 dB)
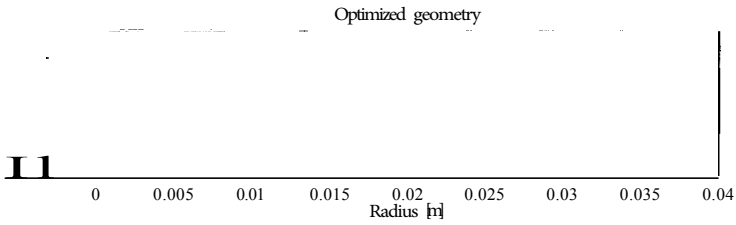
Optimized geometry

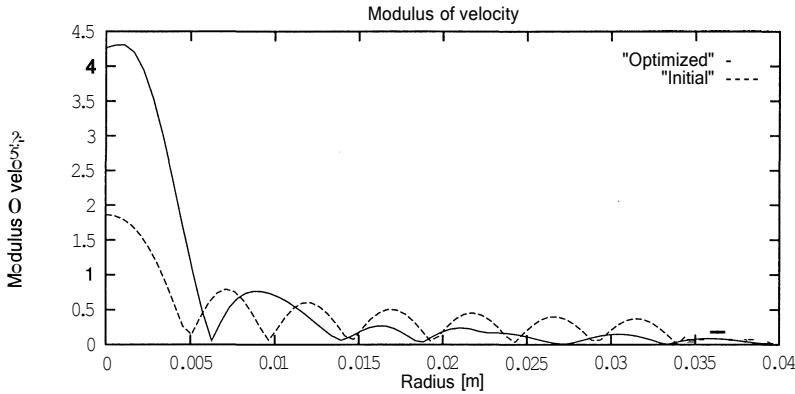Figure 13. Optimized shape, initially flat

Figure 14. Modulus of velocity initially and after optimization at 10,000 Hz
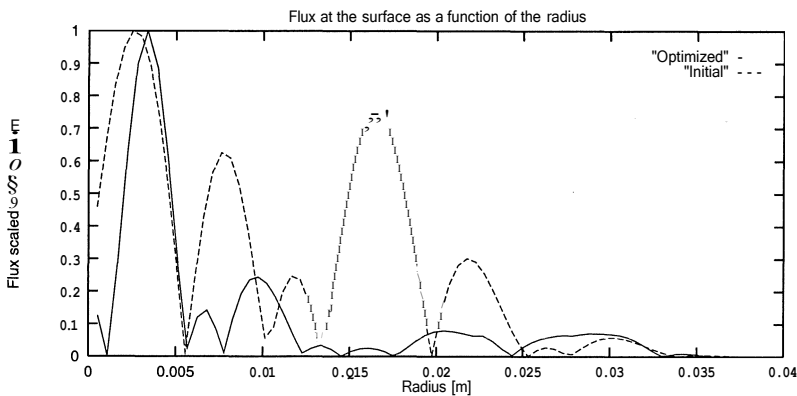

Figure 15. Flux scaled to unity, initially and after optimization

In order to compare the optimum design for the first design model in Fig. 2 whith that of the present design model (Fig. 11), we plot in Fig. 14 the modulus of velocity and in Fig. 15 the flux scaled to unity, of the optimum solution just obtained.

A comparison of Figs. 14 and 15 with the corresponding Figs. 4 and 6, respectively, shows that the optimum designs based on the first and second design model exhibit precisely the same behavioural characteristics, which may be seen as a validation of the obtained designs.

If the design which is shape optimized at the frequency of 10,000 Hz is subjected to other excitation frequencies, e.g. 1,000, 5,000, 13,000 and 15,000 Hz, see Fig. 16, the same tendency is found as in Fig. 7, namely that all the directivities are almost uniform whereas the sound pressure levels are different.

The conclusions of our investigations so far are that both the objective func-
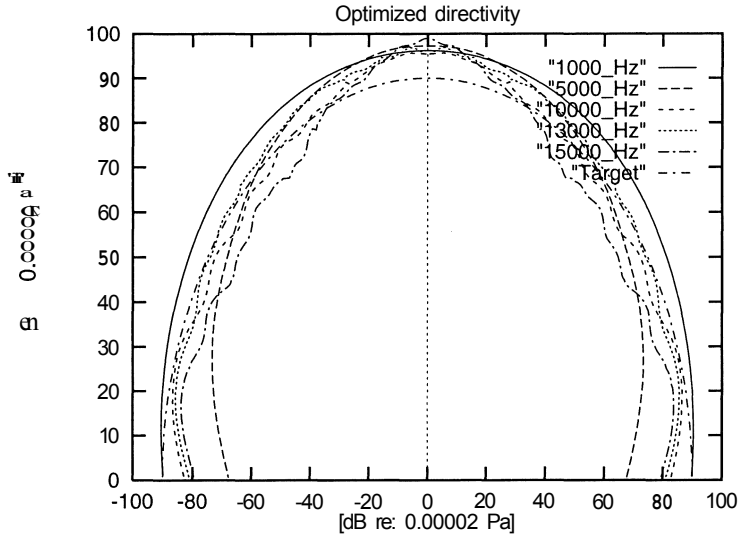
Figure 16. Directivity patterns for single frequency optimized design subjected to different frequencies

tion formulated directly relative to the directivity plot and the two design models with either discrete masses or the mid-surface shape as design variables, are well suited for yielding uniform directivity by optimization. In fact, it has been shown by optimization of two different design models that the optimum mechanism for obtaining uniform directivity is that the diaphragm acts as a point source. In the following example, a more complicated design model is presented, and the experience obtained with the previous model will be utilized.

6. Example: Shape and thickness optimization

Multifrequency optimization seems to be a good tool for elimination of change in sound pressure levels with different frequencies. Furthermore, inserting the diaphragm in a soft surround of fixed design will make it possible to increase the sound pressure levels at low frequencies. Another possibility may be to use the thicknesses of the diaphragm and of the surround as design variables, too. These augmentations have all been implemented in the design model shown in Fig. 17. As in all the preceding design models, the structure is modelled by Mindlin axisymmetric shell elements, and subjected to an external excitation force acting at the center as shown in Fig. 17. The cubic B-spline defining the shape of the mid-surface of the diaphragm is spanned by 9 points and have 8 modifiers. The circular arc between p9 and plO is the soft surround which is inserted around the diaphragm. Furthermore, the thickness of both the diaphragm and of the
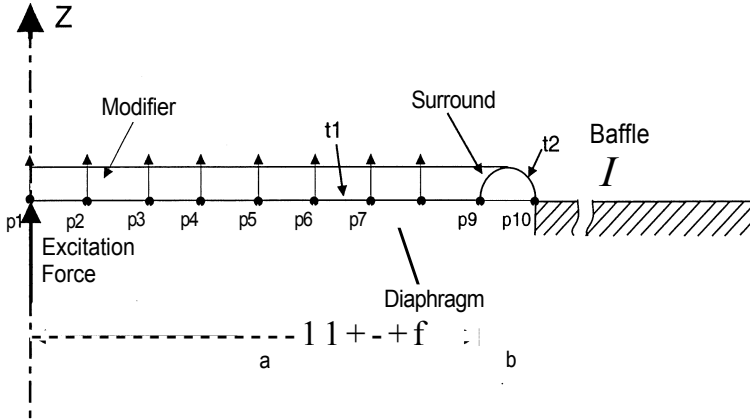
Figure 17. Design model for an initially flat diaphragm with a soft surround

surround is used as design variables (tl and t2, cf. Fig.17).

The excitation frequencies for which the diaphragm will be optimized, are chosen to be 500, 7,000 and 10,500 Hz, i.e. low, medium, and high frequency are considered. The diaphragm is surrounded by a rigid baffle. The target level for the sound pressure level is chosen to be 85 dB which is very close to the average of the initial design.

The model has additional data as given in Table 2.

Material data	Membrane	Surround
Young's Modulus E	1.5E9 N/m^2	3.0E7 N/m^2
Mass density p	600 kg/m^3	700 kg/m^3
Poisson's ratio v	0.3	0.33
Damping parameter	0.01	0.01
Model data	Membrane	Surround
initial thickness h	0.5mm	1.0mm
Num. elem. m	100	33

Table 2. Model data

The directivity results for the multifrequency optimization example are presented in Fig. 18 which shows the target curve for the sound pressure level and the directivity diagrams for the initially flat as well as for the optimized axisymmetric shell design. It is seen that, as expected, the directivities have been smoothened considerably as compared with the initial ones.

The optimized shell has a conical shape in the vicinity of the center, then a curved part and again a nearly conical shape which results in a more stiff
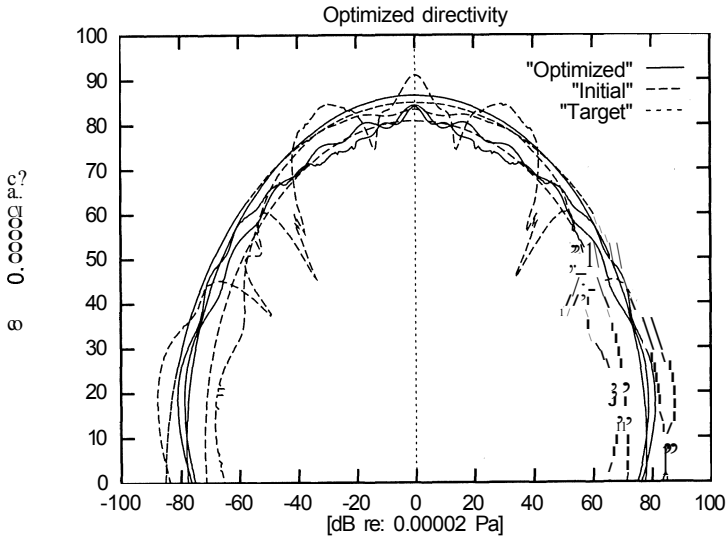
Figure 18. Directivity patterns initially and after multifrequency optimization at 500, 7,000 and 10,500 Hz (with respect to a target level of 85 dB)
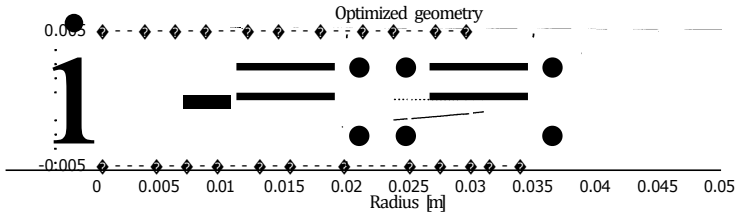

Figure 19. Optimized shape of diaphragm mid-surface

behaviour of the outer part, see Fig. 19. The thicknesses of the diaphragm and the surround which were also used as design variables, changed only slightly: the final thickness of the surround decreased from 1 mm to 0.991 mm, while the thickness of the diaphragm remained unchanged.

This example shows that it is possible to obtain a nearly uniform directivity pattern for the frequencies considered. Further tests of the optimized design when subjected to other frequencies, have shown that the directivity remains uniform. up to 13,000 Hz. However, it has been found that further improvement can be obtained if more frequencies are considered in the optimization.

7.   Conclusions

The directivity of a loudspeaker diaphragm has been optimized using as design variables the magnitudes and positions of a set of ring masses attached to the surface of the diaphragm, or the shape of the mid-surface of the diaphragm described through a quadratic B-spline.

The objective function was formulated directly to give a directivity pattern in the form of a semi-circle. However, the formulation of the objective function is very flexible and in principle it is possible to optimize the directivity towards any arbitrary shape.

The optimization of a flat circular membrane showed the possibility to obtain a uniform directivity for the entire audio frequency range, and it was found that the resulting energy flux from this membrane was concentrated around the center of the membrane, and in practice making the membrane acting like a point source. This actually ascertains that the point source is optimum for rendering the directivity uniform; this was indicated by two different design models.

The problem was then to achieve this decoupling for a wide range of frequencies. When the diaphragm is subjected to both high and low frequencies, this leads to trade-offs in the optimal design. At a low frequency, a stiff design is required to yield a reasonably high sound pressure level, whereas the uniformity of the directivity is not a problem, while at a high frequency, a soft design is required in order to make the diaphragm decoupled and to yield a uniform directivity. In order to obtain a design that offers a compromise on these requirements, a multifrequency optimization has been performed. The optimized design showed some improvement in the overall behaviour compared to a design optimized for a single frequency. However, it is believed that more frequencies should be included in the optimization if further improvements are to be obtained.

The structural vibration problem was analysed by the finite element method, while the acoustics problem was solved using the boundary element method. The size of the coupled structural acoustic equation system was reduced by usage of eigenvector synthesis for the structural modes.

The general structural optimization tool ODESSY which is being developed at the Institute of Mechanical Engineering of Aalborg University, was used as a basis for the structural analyses, and a boundary element module was developed and implemented for the acoustic analyses.

First, optimization led to a diaphragm designed such as to act essentially as a point source by placing a large mass in the inner part of the membrane, which introduced a nodal circle and decoupled the outer part of the membrane, thereby concentrating the area which radiates sound to be in the vicinity of the center. Secondly, it was shown that using the shape of the mid-surface as a design variable, it was possible to obtain a similar behaviour of the diaphragm.

Finally, the shape of the mid-surface of a diaphragm inserted in a soft sur-

round was optimized simultaneously for three different frequencies, and it was shown that it was possible to obtain a nearly uniform directivity pattern for each of these frequencies.

Acknowledgment

References

BREBBIA, C.A. and CISKOWSKI, R.D., eds. (1991) *Boundary Elements in Acoustics.* Elsevier Applied Science.

COOK, R.D. (1974) *Concepts and Applications of Finite Element Analysis.* John Wiley & Sons, Inc., second edition.

JEANS, R. and MATHEWS, I.C. (1991) Use of Lanczoz vectors in structural acoustic problems. *Structural Acoustic, ASME,* 128, 101-111.

LAMANCUSA, J.S. (1993) Numerical optimization techniques for structural-acoustic design of rectangular panels. *Computers and Structures,* 48, 4, 661-675.

LUND, E. (1994) Finite element based design sensitivity analysis and optimization. Ph.D thesis, Institute of Mechanical Engineering, Aalborg University.

MOLLER, P.M. (1993) The boundary element method for sound field calculations. Thesis, The Acoustic Laboratory, Technical University of Denmark. Report No. 55.

ST. PIERRE, R.L. JR. and KOOPMANN, G.H. (1995) A design method for minimizing the sound power radiated from plates by adding optimally sized discrete masses. *Journal of Vibration, Acoustics, Stress and Realiability in Design ASME,* 117, 243-251.

RASMUSSEN, J., LUND, E. and OLHOFF, N. (1993) Integration of parametric modeling and structural analysis for optimum design. *Proc. Advances in Design Automation, the American Society of Mechanical Engineers,* Gilmore et al., eds., Albuquerque, New Mexico, USA.

SOENARKO, B. (1993) A boundary element formulation for radiation of acoustic waves from axisymmetric bodies with arbitrary boundary conditions. *Journal of the Acoustical Society of America,* 93, 2, 631-639.

SOROKIN, V.S. (1995) Introduction to structural acoustics. Special Report No. 28, Institute of Mechanical Engineering Aalborg University, August.

TESSLER, A. (1982) An efficient, conforming axisymmetric shell element including transverse shear and rotary inertia. *Computer & Structures,* 15, 5, 567-574.

VOLLESEN, J.H. (1994) Analysis of the mechanical and acoustical properties
    of a loudspeaker unit with controlled directivity. Thesis, Bang & Olufsen
    A/S and Aalborg University, January.
Wu, T.W., SEYBERT, A.F. and LI, W.L. (1991) A coupled fem/bem formu-
    lation for fluid-structure interaction using Ritz vectors and eigenvectors.
    Structural Acoustics, NCA-Vol. 12/AMD-Vol. 128, 171-178.
Wu, T.W., SEYBERT, A.F. and LI, W.L. (1993) *Applications of the Fem and
    Bem in Structural Acoustics.* Elsevier Applied Science.